ELSEVIER

Tectonophysics 274 (1997) 83–96

TECTONOPHYSICS

Syndepositional tectonics and extension–compression relationships at the front of the Taiwan collision belt: a case study in the Pleistocene reefal limestones near Kaohsiung, SW Taiwan

O. Lacombe [a,*], J. Angelier [a], H.-W. Chen [b], B. Deffontaines [a], H.-T. Chu [b], M. Rocher [a]

[a] *Laboratoire de Tectonique Quantitative, Université P. et M. Curie, URA 1759 CNRS, Tour 26–25, E1, Boîte 129, 4 place Jussieu, 75252 Paris Cedex 05, France*

[b] *Central Geological Survey, M.O.E.A., P.O. Box 968, Taipei, Taiwan, ROC*

Received 5 February 1996; accepted 12 May 1996

Abstract

In the Kaohsiung area (SW Taiwan), large lenses of Pleistocene reef limestones interbedded in clastic layers of the Gutingkeng Formation cover the crest of the Takangshan and Panpingshan anticlines. Tectonic analyses carried out on these limestones provide evidence that these anticlines developed during deposition of the reefs. This is supported by synsedimentary normal faulting related to tensional stresses at the hinge of the anticlines. This synsedimentary extension is subperpendicular to the local trends of fold axes and parallel to the compression responsible for fold development and which is mainly marked by strike-slip faults. These observations lead us to propose a model of extension–compression relationships and reef development during Quaternary folding in the foreland of the Taiwan collision belt.

Keywords: syndepositional tectonics; compression; extension; foothills; Taiwan; reef limestones; palaeostresses

1. Introduction

A major problem in tectonics concerns the relationships between extension and compression in fold-and-thrust belts. In this paper, we describe and interpret the presence of both extensional and compressional structures at the front of the Taiwan collision belt (Fig. 1A).

A primary difficulty when addressing this problem deals with the chronological aspect of the deformation: where different tectonic mechanisms are identified in the field, it is important to determine whether they result from a polyphase evolution or not. Another important aspect concerns the relation between the geological structure and the tectonic mechanisms. For both these reasons, it is necessary to consider as a case example an area where the age of the tectonic events is tightly constrained by chronological data, the geological structure is accurately described and there is a good potential for analysing brittle tectonics.

These requirements are met in the southern segment of the outer Taiwan mountain belt, near the city of Kaohsiung (Fig. 1B). First, the stratigraphic section of this area displays young marine sedimentary series with high sedimentation rates, contrasting facies (thick mudstones and large lenses of reefal limestones) and accurate micropalaeontological dat-

* Corresponding author. E-mail: lacombe@lgs.jussieu.fr

PII S0040-1951(96)00299-5

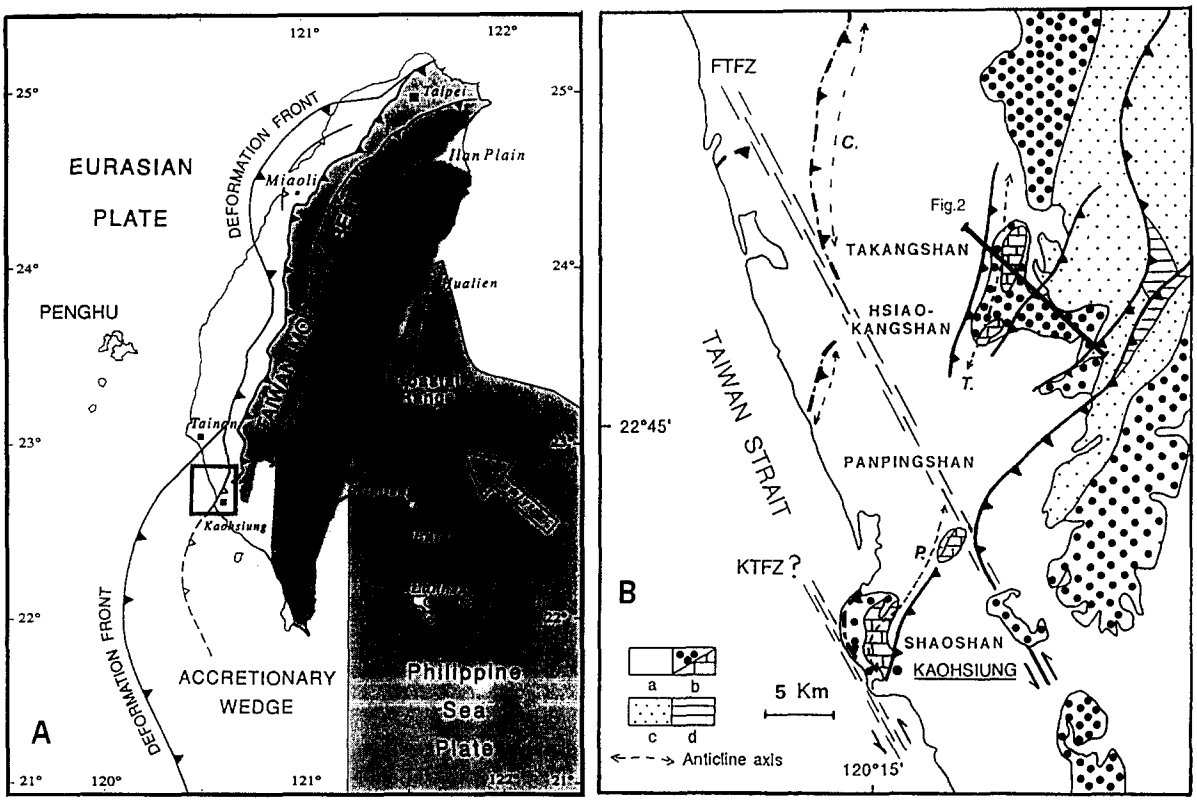

Fig. 1. (A) Geotectonic setting and main structural units of Taiwan. The large open arrow shows the present direction of convergence of the Philippine Sea plate relative to Eurasia. Heavy lines indicate major thrusts, triangles on upthrown side. *L.V.* = longitudinal valley. The frame indicates the location of the area investigated. (B) Main outcrops of reef limestones in the Kaohsiung region. *a* = Holocene; *b* = Pleistocene; *c* = Pliocene; *d* = Late Miocene. For thrusts, same key as in (A). *T.* = Takangshan anticline; *P.* = Panpingshan anticline; *C.* = Chungchou anticline. *FTFZ, KTFZ* = Fengshan/Kaohsiung Transfer Fault Zones.

ing (Chi, 1979). These series, which are affected by compressional deformation at the front of the belt, are Pliocene and Quaternary in age; the reefal limestones, which are of special interest for our study, are Pleistocene in age (Chi, 1979; Lee, 1990). As a consequence, the age of the deformation of the front units of the belt is tightly constrained, that is, Quaternary in age. Second, the geological structure of these frontal units (Fig. 1B) has been described in detail based on both geological mapping (Ho, 1986) (CPC, geological maps) and subsurface studies (Sun, 1963). Third, due to the presence of several major quarries in the reefal limestones, excellent exposures are available for tectonic analysis, and brittle features such as striated faults or tension gashes were analysed in detail. Furthermore, at microscopic scale, these limestones provide excellent material for palaeostress reconstructions based on analysis of mechanical calcite twinning (Lacombe et al., 1993; Rocher et al., 1996). Thus, the mechanisms and geometry of the major structures of these frontal belt units can be analysed and dated in detail in this particular area.

In this paper, we aim at demonstrating, based on combined stratigraphic, structural and tectonic analyses in four main sites (which correspond to monoclines near the crests of anticlines), that extension and compression do not correspond to distinct temporal events but are synchronous within the framework of propagating fold-and-thrust units in the western Foothills of Taiwan. Of particular help in this demonstration is the syndepositional tectonic record. This association between extension and compression will be discussed in the last sections of this paper.

2. Structural and sedimentary setting

The Kaohsiung region displays asymmetric folds and thrust faults that affect the thick series of Plio–Quaternary muddy and sandy sediments of the Gutingkeng Formation. The Takangshan and Panpingshan anticlines, whose axes trend NNE–SSW and NE–SW, respectively (Fig. 1B), provide good examples of such thrust-related folds. The steeply dipping (or even overturned) NW flanks of these anticlines are broken through by NW-vergent thrusts, whereas their eastern flanks dip gently toward the southeast, suggesting a fault-propagation fold type (Fig. 2). The sigmoidal virgation of the axes of these anticlines (Fig. 1B) is consistent with the occurrence of a N140° left-lateral major transfer fault zone whose offset decreases toward the deformation front, the Fengshan Transfer Fault Zone, as proposed by Deffontaines et al. (1997).

Near the top of these anticlines, thick Pleistocene reefal limestones interbedded within the clastic layers of the Gutingkeng Formation crop out (e.g., Heim and Chung, 1962; Chen et al., 1994) (Fig. 1B and Fig. 2). The lithostratigraphy and the age distribution of these limestones have been analysed in detail (Chi, 1979, 1989; Lee, 1990) and are summarized in Fig. 3; the age of the reefs ranges from 1.2 to 0.45 Ma, and is younger from south (Kaohsiung) to north (Takangshan).

The Takangshan and Hsiaokangshan reef limestones are located on the eastern limb of the Takangshan anticline, whereas the Panpingshan and Kaohsiung limestones are located on the eastern limb of the Panpingshan anticline. On these eastern flanks the bedding dips about 20° on average to the east-southeast. Seismic reflection profiling carried out by the Chinese Petroleum Corporation (Sun, 1963) has allowed identification of these structures at depth (Fig. 4). The survey shows good reflections corresponding to synclines and to the flanks of the Takangshan, Panpingshan and Chungchou anticlines (Fig. 1B). These strong reflections correlate well to the attitudes of the reef limestones in the subsurface. The limestones of Takangshan and Hsiaokangshan may thus be correlated with the limestones of Panpingshan and the upper part of the Kaohsiung limestones (Sun, 1963).

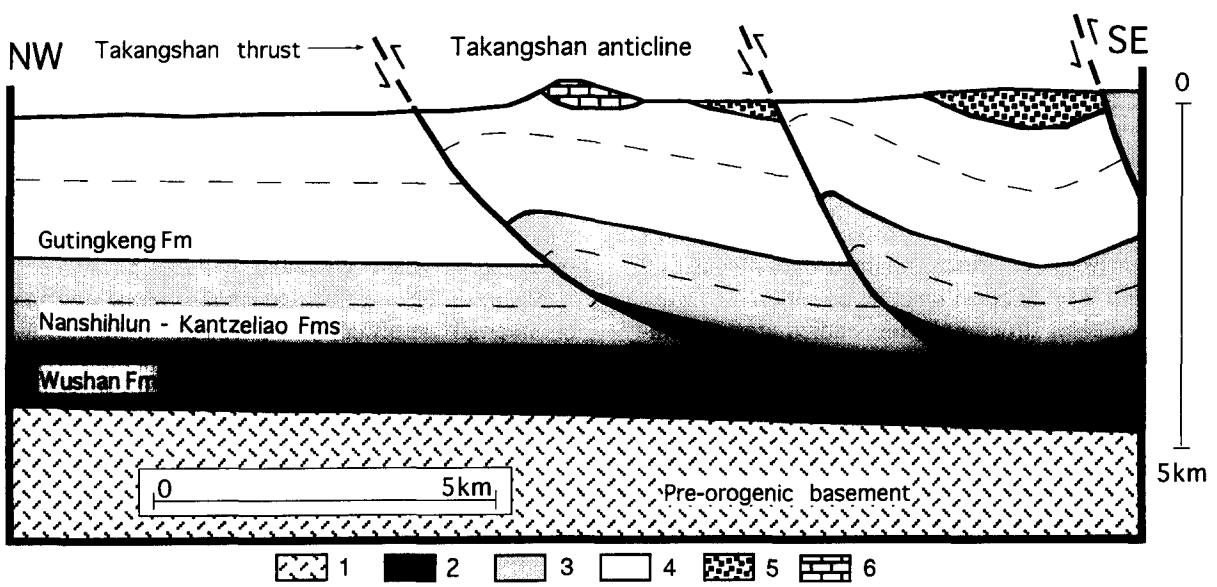

Fig. 2. Geological cross-section through the Takangshan anticline (see location in Fig. 1B). Note the particular location of the reefs and the fault-propagation fold geometry. *1* = pre-orogenic basement; *2* = Wushan Fm (Miocene) = decollement level; *3* = Nanshihlun–Kantzeliao fms (Pliocene); *4* = Gutingkeng Fm (Pleistocene); *5* = Erchungchi Fm (Pleistocene); *6* = reef limestones (Pleistocene) interbedded within the upper Gutingkeng Fm. The Holocene series overlying the Gutingkeng and Erchungchi formations have not been represented (after Mouthereau, 1995, unpubl. data).

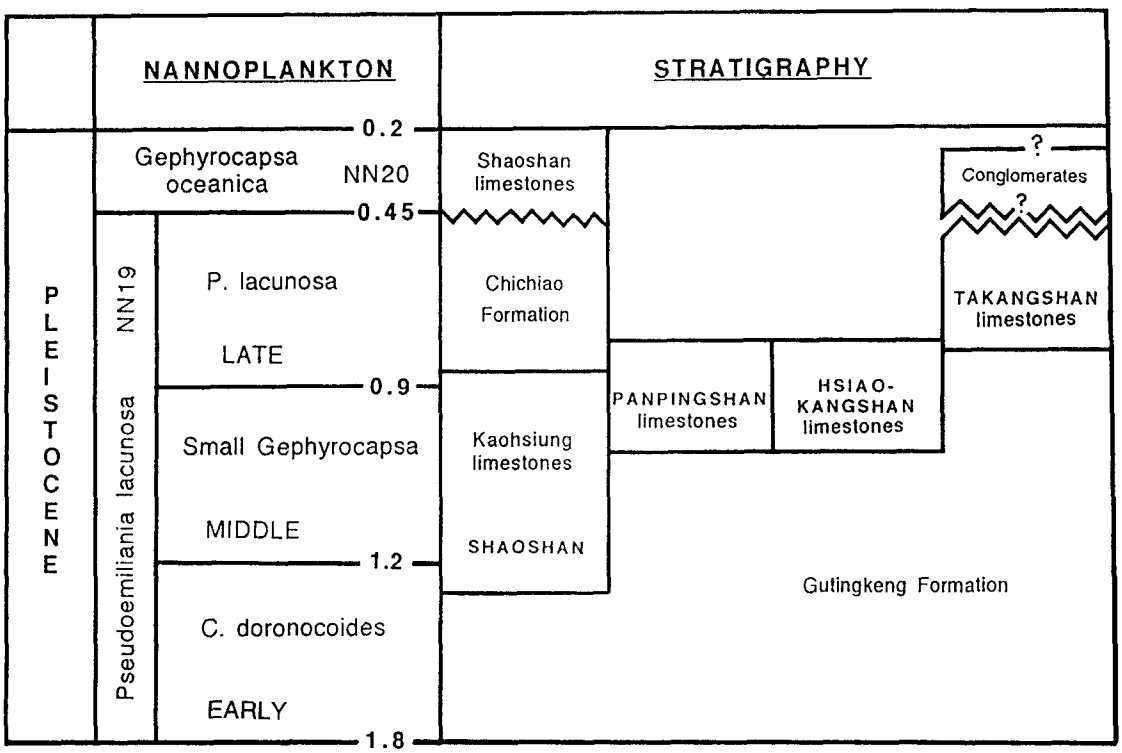

Fig. 3. Age of investigated reef limestones. Strata were dated (NN19 and NN20 zones) with nannoplankton data (Chi, 1979, 1989; Lee, 1990).

3. Method for tectonic analysis

Although it is not necessary here to describe in detail the brittle tectonic analysis carried out, it is worthwhile to briefly summarize the principles of such an analysis, which combines consideration of (1) the major structures, (2) palaeostress reconstructions, and (3) syndepositional deformation.

The general structure of the studied area is dominated by the presence of major folds, thrusts and strike-slip faults which have been described previously based on geological mapping and subsurface studies (Fig. 1BFigs. 2 and 4). Medium-size structures, especially strike-slip faults and normal faults, are observable in large quarries within the reef limestones (Fig. 5). In order to reconstruct tectonic mechanisms, computation of palaeostress tensors was systematically undertaken based on fault-slip data. The computer-based inversion method used in this study is that of Angelier (1984). The results are the orientations (trends and plunges) of the three principal stress axes σ_1, σ_2, σ_3 and the Φ ratio between principal stress differences $[\Phi = (\sigma_2 - \sigma_3)/(\sigma_1 - \sigma_3)]$ (Table 1). Additional information is obtained from stylolites, tension gashes and joints. The procedure for separating successive stress tensors and related subsets of fault-slip data is based on mechanical reasoning (e.g., Angelier, 1984) and relative chronology observations where available.

Because the reef limestones also show evidence of internal deformation by calcite twinning, we also conducted palaeostress reconstructions based on computer inversion of mechanical calcite-twin data (Lacombe et al., 1993; Rocher et al., 1996), using the method described by Laurent (1984) and Etchecopar (1984). The twin data were collected from large xenomorphic calcite crystals with random crystallographic orientation resulting from recrystallization of primary coralline aragonitic material. We combined both methods in order to identify the stress patterns related to the Quaternary tectonic evolution of the frontal units of the belt.

Dating of the recognized tectonic events additionally requires stratigraphic information about

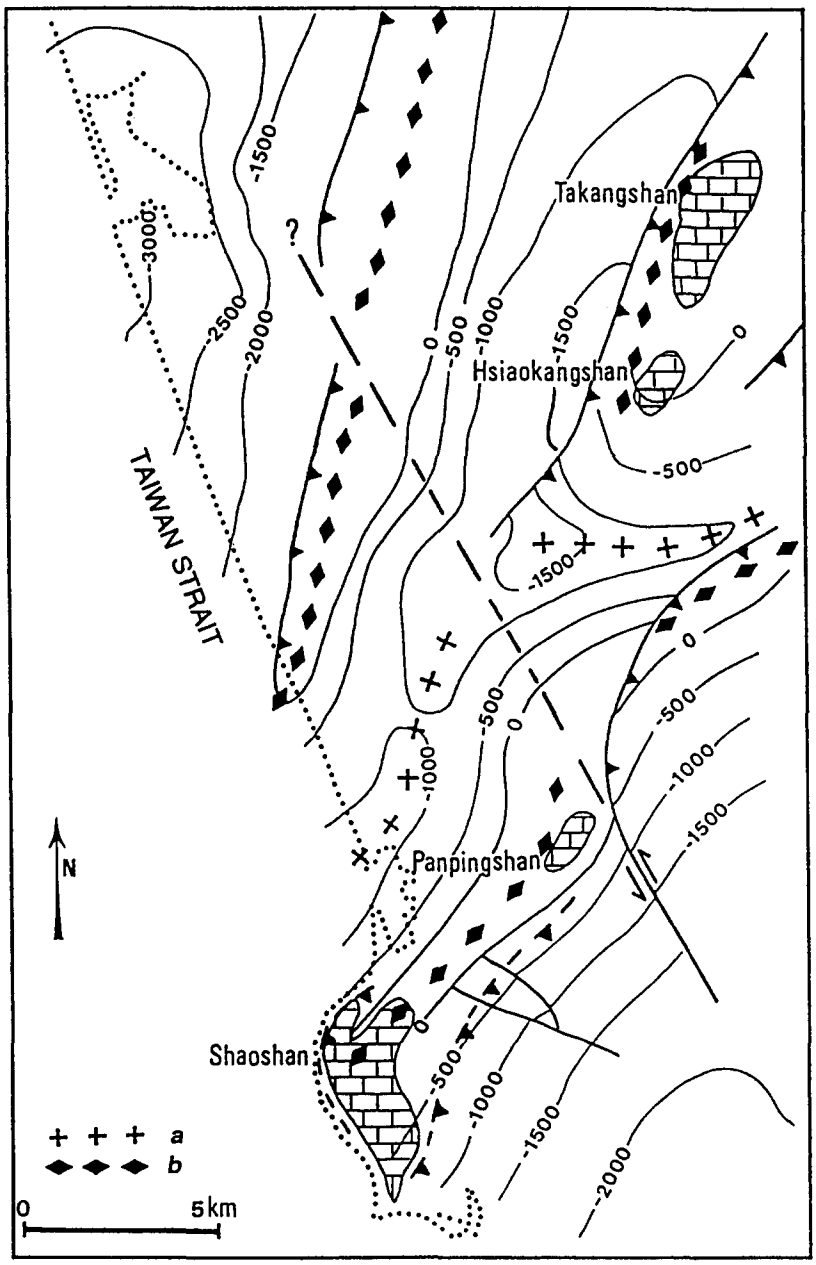

Fig. 4. Structural contour map of the reflection horizon on the top of the Kaohsiung limestone and the limestone of Panpingshan and the corresponding reflection horizon showing the stratigraphic relationships between limestones (modified from Sun, 1963). Values are in meters. *a* = syncline; *b* = anticline. Dotted line represents shoreline. For thrusts, same key as in Fig. 1.

deformed units and/or evidence of syndepositional tectonism. Relative tectonic chronology data (e.g., cross-cutting relationships between faults or superimposed striations on fault surfaces) were combined with such observations. Based on the assumption that the structural style and the palaeostress orientations remain nearly homogeneous for a given tectonic event, we have attempted to reconstruct the chronological relationships between the tectonic regimes identified.

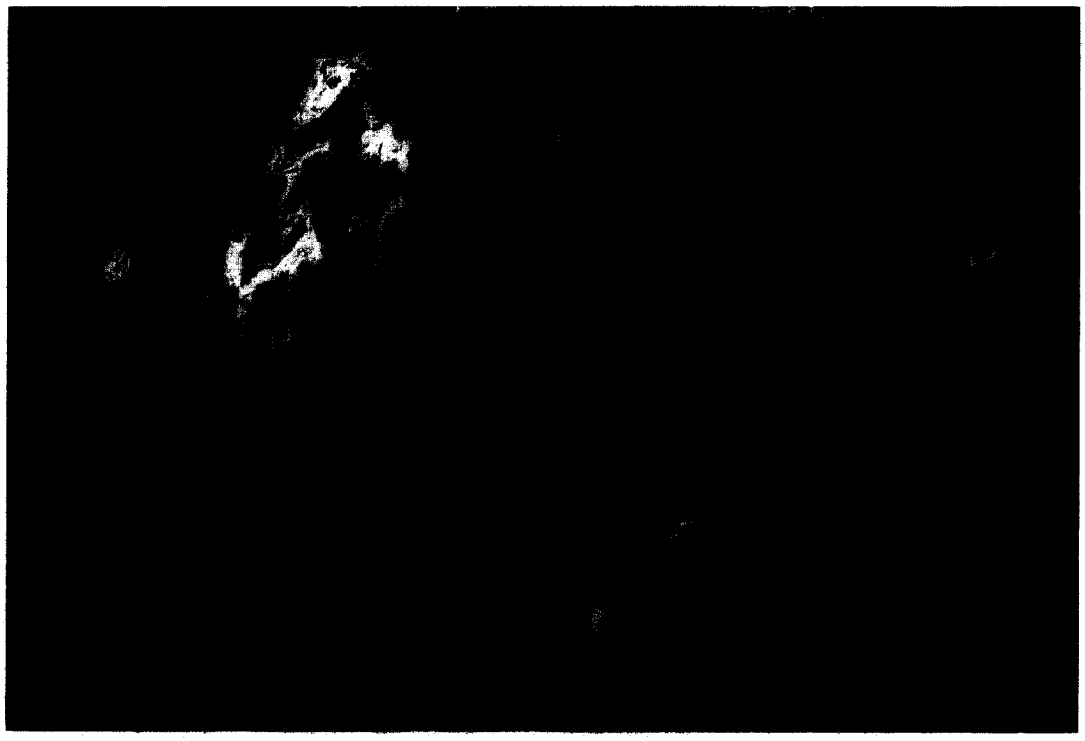

Fig. 5. Example of minor strike-slip fault observed within the reef limestones.

Table 1
Results of stress tensor determination based on fault-slip data

Site	Ref.	σ_1	σ_2	σ_3	Φ	F	α	Q
Takangshan	T1	288 (74)	066 (12)	158 (10)	0.18	9	15.7	A
	T2	127 (17)	324 (72)	218 (05)	0.52	23	11	A
	T3	274 (03)	037 (84)	288 (74)	0.08	89	10	A
Hsiaokangshan	H1	148 (70)	016 (14)	283 (03)	0.35	5	1	B
	H2	270 (04)	029 (81)	179 (08)	0.06	46	14.4	A
Panpingshan	P1	334 (72)	236 (03)	145 (18)	0.36	11	14	A
	P2	132 (02)	011 (87)	222 (03)	0.00	30	14.5	A
Shaoshan	S1	037 (01)	304 (77)	127 (13)	0.02	67	10.8	A
	S2	025 (69)	192 (21)	284 (04)	0.24	22	13.5	A
	S3	131 (03)	338 (87)	221 (02)	0.30	36	14.1	A
	S4	253 (03)	101 (86)	343 (02)	0.17	12	9.7	B

Trend (and plunge) of each stress axis, in degrees; Φ defined in text; F = number of faults consistent with the tensor; α = average angle between actual and calculated striations, in degrees; Q = quality of the tensor (A to D) estimated according to the number of faults explained, the variety of their orientations and the α value. For diagrams corresponding to the determined stress tensors, see Fig. 7.

Special attention was paid to external rotations of studied rock masses due to folding: reconstruction of the original attitudes of minor structures and related palaeostress axes with respect to fold axes and bedding attitudes may allow separation of data subsets based on their age relative to fold development.

4. Results—major tectonic regimes

In this section, we describe the main tectonic regimes identified in the field based mainly on the analysis of fault systems within the reef formations and their interpretation in terms of stress.

4.1. Syndepositional extension

As an example of a sedimentary feature related to extensional tectonics, we describe in the Panpingshan limestone a graben-related palaeochannel, which can be observed along a quarry scarp trending parallel to the fold axis (Fig. 6A). In the upper layer of the section, the channel is filled by thick rhodolith limestones. It seals a small graben filled by mudstones (Fig. 6). The northeastern border of the graben corresponds to a fault plane dipping steeply to the south and striking nearly E–W. Slickenside lineations on this fault plane indicate a normal movement with a minor left-lateral component (Fig. 6B). We conclude that the normal fault slip locally controlled the location of the channel, and therefore that normal faulting played a significant role during deposition and building of the Pleistocene reef.

Other normal faults trending N060° to E–W and dipping gently to the north or steeply to the south at Panpingshan are mechanically consistent with the syndepositional normal fault described above. They generally correspond to a N140° extension (Fig. 7, diagram P1). The calculated stress tensor displays a σ_2 axis nearly parallel to the bedding (and hence to the anticline axis); the σ_3 axis trends perpendicular to bedding strike but is not horizontal and plunges less than the bedding dip (Fig. 7, diagram P1). We conclude that normal faulting occurred during folding, probably in response to tensile stresses at the hinge of the anticline (extrados effect).

In Takangshan, some normal faults are also observable, indicating a NW–SE extension (Fig. 7, diagram T1). Tension gashes associated with these normal faults, showing mudstone infill, suggest that extension occurred during sedimentation (at least prior to lithification).

In the Shaoshan quarry, normal faults and tension gashes clearly correspond to a N120° direction of extension (Fig. 7, diagram S2). A system of N–S- to N020°-trending right-lateral strike-slip faults and N040° to N060°-trending left-lateral strike-slip faults was also identified, corresponding to a similar direction of extension (N130°; Fig. 7, diagram S1). This similarity of σ_3 trends suggests that a single, synfolding extension is responsible for both these strike-slip faults and the normal faults through a permutation between σ_1 and σ_2 axes.

Calcite-twin analysis also provides evidence for nearly NW–SE extensional stresses (Rocher et al., 1996). This NW–SE extension seems to be associated in some sites with a slight NE–SW compression,

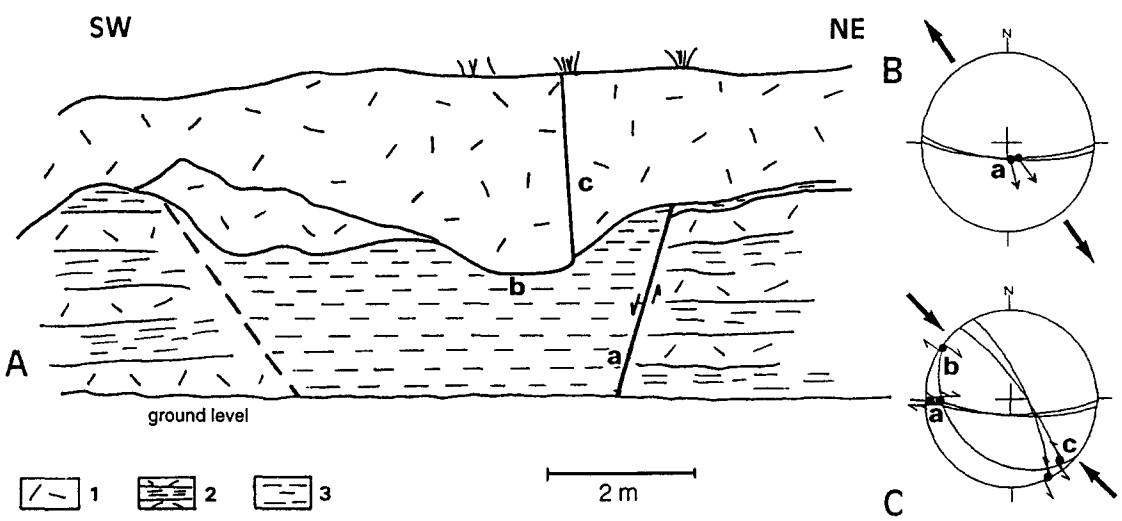

Fig. 6. Schematic sketch of synsedimentary normal fault and related palaeochannel in the Panpingshan quarry. *1* = limestones (rhodolith rudstones/alternating coral limestones–mudstones); *2* = bioclastic beds alternating with mudstones; *3* = mudstones. Diagrams: thin curves represent fault planes, and dots with double arrows (left- or right-lateral) or simple ones (centrifugal-normal) indicate slickenside lineations. *a*, *b*, *c* represent striated fault surfaces observed in the field. Note that plane *a* exhibits two superimposed striations. The arrows on diagrams (B) and (C) correspond to the stress orientations determined using stress tensor calculation (see Fig. 7 and Table 1).

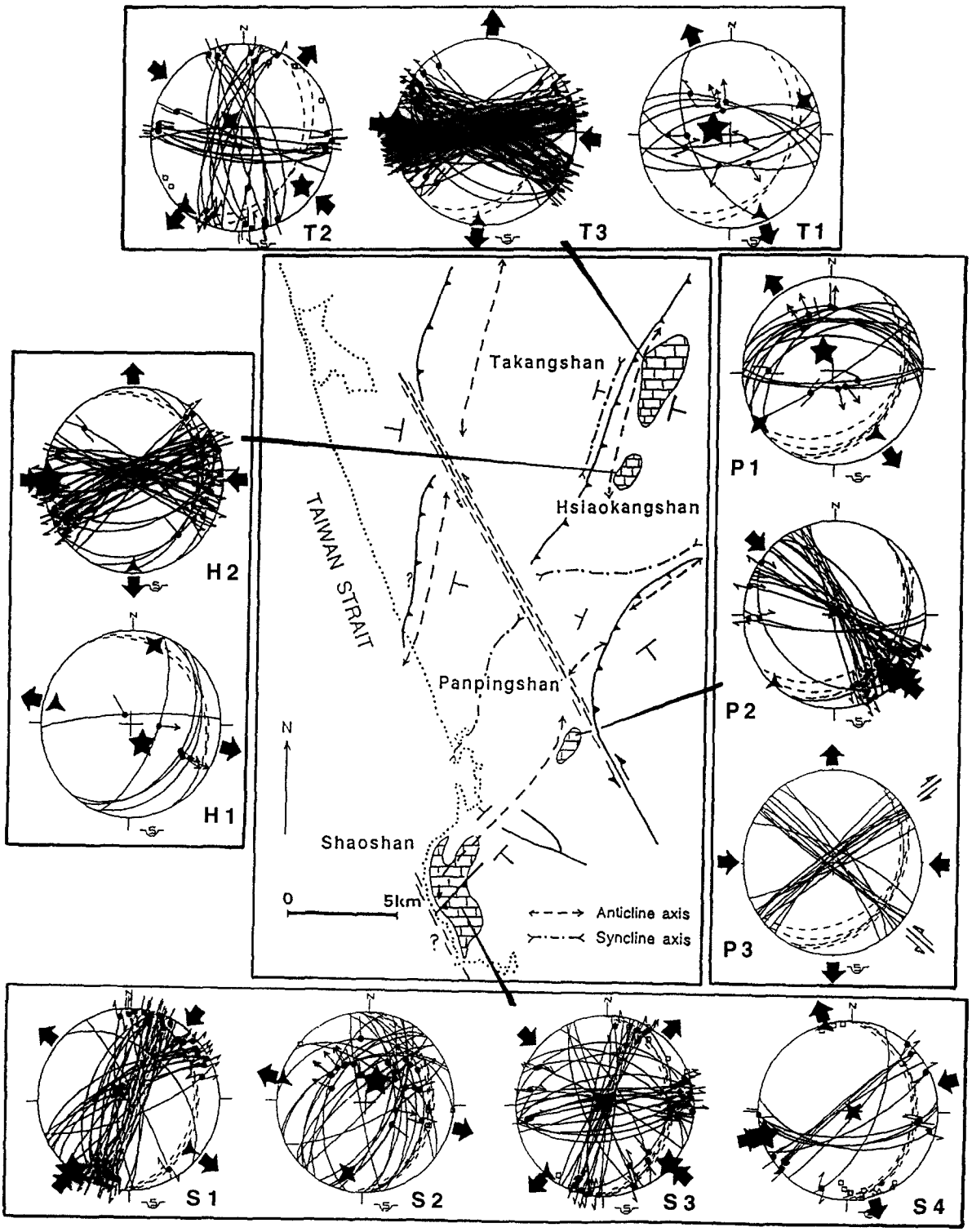
T2
T3
T1
Takangshan
Hsiaokangshan
TAIWAN STRAIT
Panpingshan
Shaoshan
N
0
5km
Anticline axis
Syncline axis
H2
H1
P1
P2
P3
S1
S2
S3
S4

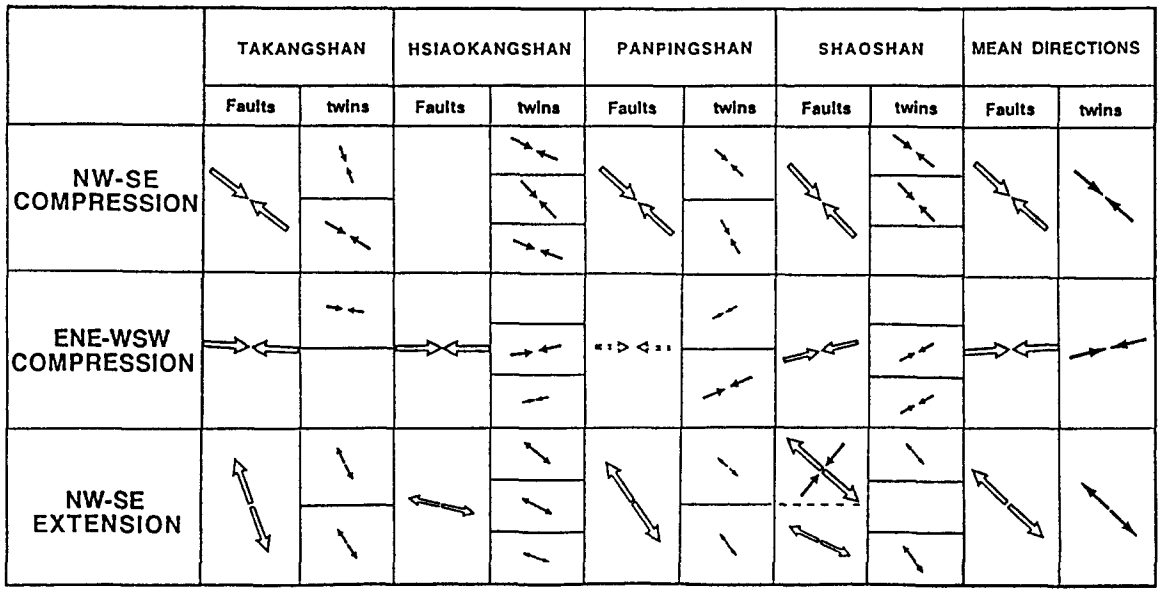

Fig. 8. Summary of compressional (σ_1 = convergent arrows) and extensional stress trends (σ_3 = divergent arrows) determined from inversion of calcite-twin data (solid arrows: Rocher et al., 1996) and fault-slip data (unfilled arrows: this work). The larger the size of the arrows, the better the quality of results. Last two columns: average directions of NW–SE compression, ENE–WSW compression, and NW–SE extension, obtained from twin and fault analyses.

also suggesting σ_1/σ_2 permutation, σ_3 axis remaining oriented N130° (Fig. 8).

Summarizing, the investigated reef limestones show evidence of early extensional deformation marked by normal faults and tension gashes. These extensional features were preserved and could be reliably recognized in the reef limestones because of both the relatively well-lithified nature of reef limestones at very shallow depths (even at the sediment surface, in contrast to surrounding mudstones), and the geometry of the free surface provided by the protrusion of the reef above the surrounding surface by the fault-propagation geometry, coupled with rapid vertical reef growth. Although these normal faults show dispersion in trend relative to the orientation of the fold axes, partly due to the inhomogeneity of reef rock masses, all the sites provide evidence of a mean NW–SE direction of extension (Fig. 7). The direction of the σ_2 axes of the calculated stress tensors is generally roughly parallel to that of the anticline axes, so that this extension is very probably related to fold development. Considering both the synsedimentary character of normal faulting and its relation to fold structure development, we conclude that the folds formed during the deposition of the Pleistocene mudstones and limestones.

4.2. Compressions

In the Panpingshan quarry, left-lateral strike-slip faults trending N150° to N160° and right-lateral strike-slip faults trending N110° to N130° indicate a N140° compression (Fig. 7, diagram P2). This compression is perpendicular to the fold axis and related to folding. The slip vectors on these strike-slip faults, as shown by slickenside lineations, display a variety of orientations, ranging from parallel to bedding to horizontal; this suggests that such strike-slip fault-

Fig. 7. Results of stress reconstruction based on fault-slip analysis on reef limestones of SW Taiwan. Fault-slip data: as in Fig. 6, thin curves represent fault planes, and dots with double arrows (left- or right-lateral) or simple ones (centrifugal-normal; centripetal-reverse) indicate slickenside lineations. Stars indicate stress axes with five points (σ_1), four points (σ_2) and three points (σ_3). Small squares represent poles to tension gashes. Bedding planes shown as dashed lines. *T*, *P*, *S*, *H* and related numbers refer to tensors of Table 1.

ing probably occurred contemporaneous with folding (the slickensides of the earliest strike-slip faults being tilted as for the bedding, those of the latest ones being horizontal). Two systems of large subvertical fractures were also measured, which probably correspond to conjugate strike-slip faults related to a nearly E–W compression, although striations are absent (Fig. 7, diagram P3).

In the Shaoshan quarry, a N130° compression has also been identified, marked in the field by both strike-slip and reverse faults (Fig. 7, diagram S3). A few tension gashes and strike-slip faults additionally indicate a N080° compression (Fig. 7, diagram S4). The main N130° compression identified in Panpingshan and Shaoshan is perpendicular to the average trend of the Panpingshan anticline (Figs. 1 and 7).

In Hsiaokangshan, most of the measured strike-slip faults are consistent with an E–W compression (Fig. 7, diagram H2), which is subperpendicular to the local N–S to N020° trend of the axis of the Takangshan anticline.

In Takangshan, two different systems of strike-slip faults could be identified. The first set is similar to the system of strike-slip faults identified in Hsiaokangshan and is also related to a nearly E–W compression which is subperpendicular to the local N020° trend of the axis of the Takangshan anticline (Fig. 7, diagram T3). The second set comprises conjugate right-lateral E–W strike-slip faults and left-lateral N160° to N200° strike-slip faults associated with N130°-trending tension gashes; these structures are consistent with a N130° compression (Fig. 7, diagram T2). The calculated σ_1 axis being not horizontal but dipping less than the bedding, we conclude that this compression occurred during folding, as already suggested for the NW–SE compression in Panpingshan. The Takangshan quarry also displays evidence of karst development in relation to uplift and emergence of the reefs. The karst deposits consist mainly of red clays, which have filled the former faults and tension gashes. Some strike-slip faults (N–S- to N020°-trending sinistral strike-slip faults) affect these red clays, suggesting the late occurrence of the N130° compression. This suggests that the N130° compression occurred during and after folding and reef development.

Calcite-twin analysis also provides evidence that the reef limestones underwent a compressional stress history. The results consistently reveal a NW–SE compression with vertical σ_2 axis and a nearly E–W compression with vertical σ_3 axis (Fig. 8). The best record corresponds to the NW–SE compression, which was identified in all the sites (Rocher et al., 1996).

Summarizing, the palaeostress orientations calculated from both minor fault patterns and calcite-twin data (Fig. 8) consistently reveal a NW–SE compression (N131° from twins and N128° from faults on average), a NW–SE extension (N133° and N127°), and a nearly E–W compression (N077° and N086°). Moreover, most twins developed in response to stress regimes with subvertical σ_2 or σ_3 axes, which suggests that these stress regimes are predominantly compressional, in agreement with field observations of strike-slip faults associated with reverse faults and fold-and-thrust systems.

5. Chronological and geometrical relationships between extension and compression

Relative chronology criteria such as cross-cutting relationships between faults or superimposed striations on fault surfaces allow reconstruction of the sequence of extension and compression. In Takangshan, some of the nearly E–W-trending normal faults were reactivated as right-lateral strike-slip faults. Similar observations were made in Hsiaokangshan and Panpingshan. In Panpingshan, the syndepositional normal fault displays a secondary set of subhorizontal slickensides, indicating its reactivation as a dextral strike-slip fault. The edge of the limestone channel has also been reactivated as a right-lateral/reverse fault (Fig. 6C); finally, the channel is cross-cut by a N150°-trending left-lateral strike-slip fault. All these features are consistent with a N140° compression postdating syndepositional extension (Fig. 6C).

In Shaoshan, some of the N020° right-lateral strike-slip faults related to the synfolding extension have been reactivated as left-lateral strike-slip faults consistent with the N140° compression (Fig. 7).

These observations indicate that (1) at least part of the NW–SE extension occurred early, before development of compressional brittle features, and (2) both the extension and the NW–SE compression occurred nearly synchronous with folding. However,

the chronological criteria do not allow to draw definite conclusion concerning the succession of NW–SE and E–W compressions, suggesting a complex evolution.

The identification of two compressional states of stress in the Pleistocene strata is a surprising result because monophase compressional tectonism is expected in such young series. This reveals that complex deformation occurred during a brief time span. When comparing the results to available palaeostress reconstructions from Pleistocene units on the whole island of Taiwan (Angelier et al., 1986; Chu, 1990), the Kaohsiung region clearly displays a heterogeneous, disturbed stress field, in contrast to the rather homogeneous WNW–ESE compressional trends in other regions. This heterogeneous stress distribution during the Quaternary cannot be consistently explained in terms of successive events: it should rather be explained by local perturbation and reorientation of the regional compression. The Kaohsiung area exhibits a complex system of folded–faulted blocks separated by major thrusts, strike-slip faults and transfer faults that affect the Pleistocene rocks (Sun, 1963; Deffontaines et al., 1997). This structural pattern provides a key for interpreting the deviation of the regional compression during the Quaternary in SW Taiwan: as already proposed (Lacombe et al., 1995; Rocher et al., 1996), the regional compression has probably suffered strong local reorientation during the structural evolution of the fold-and-thrust units, resulting in a stress component oriented NW–SE nearly perpendicular to the fold axes and nearly parallel to the N140°-trending Fengshan Transfer Fault Zone, and in an ENE–WSW to E–W compression oblique at large angle to the N140° left-lateral wrench fault zone (Fig. 7). According to this interpretation, these compressions probably followed each other (or alternated) quickly in the Kaohsiung region during the Pleistocene, and thus should not be interpreted in terms of two events.

Considering that alternating occurrence of NW–SE and nearly E–W compression during the Pleistocene reflects stress–strain inhomogeneity, a crucial question concerns the homoaxiality of the σ_1 and σ_3 axes reconstructed from compressional and extensional structures. The reconstructed σ_1 axis trends nearly perpendicular to the local trend of anticline axes, which is also the case for the σ_3 deduced from synsedimentary normal faulting. This suggests that compression and extension are probably synchronous and both related to fold development. The extension, parallel to the main compressive stress and perpendicular to fold axes, thus probably corresponds to a local extrados effect: during folding, tension at anticline hinges (where the reefs developed) was large enough to result in the development of tension cracks and normal faults. We thus conclude that these apparently contrasting stress regimes are related to a single overall mechanism: the development of a fold-and-thrust unit at the front of a mountain belt.

6. Tentative model of extension–compression relationships and reef development during folding

A model of the evolution of Pleistocene deformation and stress in SW Taiwan is proposed in Fig. 9, based on consideration of the structural geometry of a fault-propagation fold reference and observed variation in stress regimes during folding.

Reefs developed on top of structural highs raised by folding (Gong et al., 1995), presumably related to a west-vergent thrust (Fig. 9A, stage a), under a regional compressional state of stress (σ_3 vertical). On such highs, decreasing clastic flow induced favourable palaeoecological conditions for reefs to grow. The lower part and the fringes of the reef are thus interbedded with mud. Continuing folding due to westward-propagating thrusting allowed the growth of the reefs. During reef development, local synfolding extension occurred nearly perpendicular to fold axis (Fig. 9A, stage b), in response to tensile stresses at the hinge of the anticline. The regional compressional state of stress (σ_3 vertical) thus changes within the reefs to local extensional state of stress (σ_1 vertical), the σ_2 axis of the stress tensor remaining nearly parallel to fold axis (permutation of σ_3 and σ_1 axes). This extension is marked by synsedimentary tension gashes and normal faults. An additional eastward migration of the climax of reef development can be envisaged at this step due to the asymmetry of the fault-propagation fold, as well as some collapse along the eastern flank of the fold.

Reefs developed until they reached water level and emerged. At this step, folding progressively

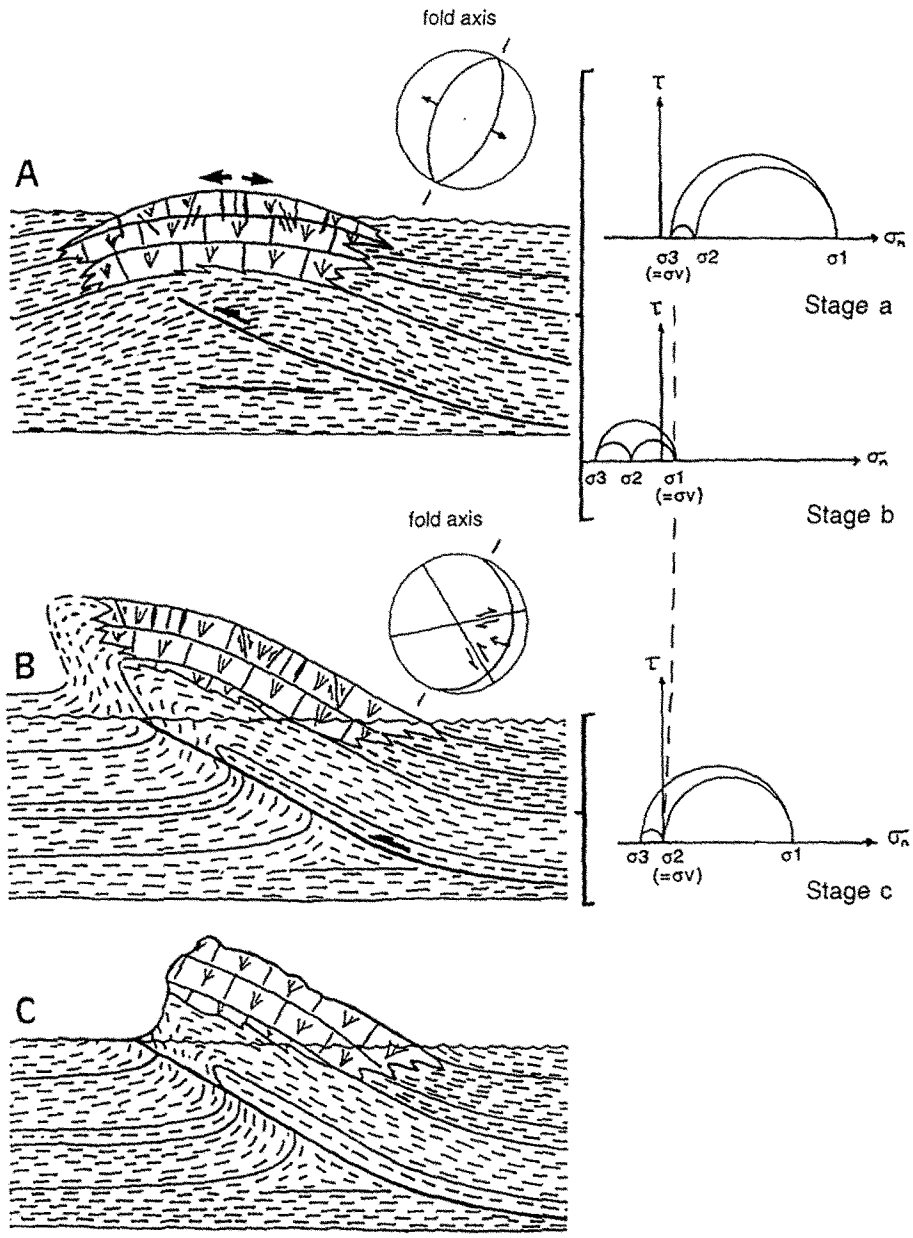

Fig. 9. Tentative model of extension–compression relationships and reef development during folding. The diagrams illustrate schematically the tectonic structures which developed at each stage within the reef limestones; the dimensionless Mohr circles illustrate the evolution of the stress regime during folding (*stages a, b, c*). (A) Reefs developed on top of structural highs raised by folding, presumably related to a west-vergent thrust. Continuing folding due to westward-propagating thrusting in response to regional compression at nearly N110° (Angelier et al., 1986) allowed growth of reefs, under a regional compressional state of stress (σ_3 vertical) (stage a). Local synsedimentary extension, nearly perpendicular to fold axis, occurred in response to tensile stresses at the hinge of the anticline: the regional compressional state of stress (σ_3 vertical) thus changes within the reefs to local extensional state of stress (σ_1 vertical), the σ_2 axis of the stress tensor remaining nearly parallel to fold axis (permutation of σ_3/σ_1, with magnitude of the vertical stress σ_v remaining nearly constant: stage b). (B) Reefs developed until they reached sea level and emerged. At this step, presumably folding slowed down then ceased and shortening (E–W to NW–SE compression) was achieved mainly by strike-slip faulting (regional compressional state of stress with σ_2 vertical, the fold axis being now parallel to the σ_3 axis). The magnitude of the vertical stress is expected to have decreased due to synfolding erosion, mainly between stage b and stage c. (C) Syn- and post-folding erosion results in the present morphology of the Takangshan, Hsiaokangshan, Panpingshan and Shaoshan hills.

slowed down then ceased (the thrust propagated towards a more external ramp, the Chungchou fault) and shortening in the reefs was achieved mainly by strike-slip faulting (regional compressional state of stress with σ_2 vertical, the fold axis being now parallel to σ_3 axis; Fig. 9B, stage c). At the same time, syn- and post-folding erosion presumably caused decrease in magnitude of the vertical stress (σ_3 axis in stage a, σ_1 axis in stage b, σ_2 axis in the latest stage c) and produced the present-day morphology of the Takangshan, Hsiaokangshan, Panpingshan and Shaoshan hills covered by reef limestones (Fig. 9C). This erosion, which was presumably more important at the top and along the steep flank of the anticline, has removed the poorly consolidated muddy and sandy sediments of the Gutingkeng Formation more easily than the reef limestones. Both this erosion and the possible migration of zones of reef growth in response to propagating folds may explain that reefs are now found located on the eastern limbs of the folds. Emergence of the reef was accompanied by karst development (at Takangshan, for example), marked by local dissolution of the limestones and deposition of red clays within cavities and former fractures.

7. Conclusion

The model that we propose for the Pleistocene tectonic–sedimentary evolution in SW Taiwan, based on careful consideration of tectonic–sedimentary relationships, shows that compression, extension and folding may occur nearly simultaneously (Fig. 9). We suspect that such associations are common in the forelands of fold-and-thrust belts, although in most cases stratigraphic evidence does not allow accurate determination of extension–compression complementarity. We conclude that careful consideration of multiple stress regimes is indispensable, because they may not reflect independent events.

Another important point concerns the age of the fold–thrust kinematics in SW Taiwan. Because reefs developed in response to thrust-related folding, the age of the reefs allows dating of the westward kinematics of the frontal units. The northward-decreasing age of the reef formations, which is somewhat inconsistent with the general southward migration of the collision (Suppe, 1984) could possibly be related to a late differential displacement of thrust sheets along the Fengshan Transfer Fault Zone and/or to the influence of the topography of the basement of the margin which controls the propagation of the frontal units.

Acknowledgements

The work was supported by the French Institute of Taipei–National Science Council of Taiwan cooperation framework, by the Central Geological Survey of Taiwan, and by the Institut Français du Pétrole. The authors would like to thank Prof. H.-H. Tsien from the National Taiwan University for discussions about development of reefs, and Dr. Neil Lundberg, Dr. Philippe Laurent and an anonymous reviewer for their constructive comments on the paper.

References

Angelier, J., 1984. Tectonic analysis of fault slip data sets. J. Geophys. Res., 89(B7): 5835–5848.

Angelier, J., Barrier, E. and Chu, H.T., 1986. Plate collision and paleostress trajectories in a fold–thrust belt: The Foothills of Taiwan. Tectonophysics, 125: 161–178.

Chen, H.W., Wu, L.C. and Tsien, H.H., 1994. The contact relationship between the Early Pleistocene Panpingshan Limestone and Gutingkeng Formation in the Kaohsiung area, southern Taiwan. Central Geol. Surv. Spec. Publ., 8: 101–119 (in Chinese).

Chi, L.-M., 1989. Sedimentological study of limestones at southern Shoushan, Kaohsiung. Master thesis, National Sun Yat-Sen University, Kaohsiung, Taiwan (in Chinese).

Chi, W.R., 1979. A biostratigraphic study of the late Neogene sediments in the Kaohsiung area based on calcareous nannofossils. Proc. Geol. Soc. China, 22: 121–144.

Chu, H.-T., 1990. Néotectonique cassante et collision plio–quaternaire à Taiwan. Thèse de Doctorat-ès-Sciences, Univ. P. et M. Curie, Paris, Mém. Sci. Terre, 90-28, 292 pp.

Deffontaines, B., Lacombe, O., Angelier, J., Chu, H.-T., Mouthereau, F., Lee, C.-T., Deramond, J., Lee, J.-F., Yu, M.-S. and Liew, P.-M., 1997. Quaternary transfer faulting in Taiwan Foothills: evidence from a multisource approach. In: S.E. Lallemand and H.-H. Tsien (Editors), Active Collision in Taiwan. Tectonophysics, 274: 61–82 (this issue).

Etchecopar, A., 1984. Etude des états de contraintes en tectonique cassante et simulation de déformations plastiques (approche mathématique). Thèse de Doctorat-ès-Sciences, Univ. Sci. Techn. Languedoc, Montpellier, 270 pp.

Gong, S.-Y., Lee, T.-Y., Wu, J.-C., Wang, S.-W. and Yang, K.-M., 1995. Possible links between Plio-Pleistocene reef development and thrust migration in the southwestern Taiwan. Symp. 'Active Collision of Taiwan', 22nd–23rd March, Taipei, Taiwan, pp. 113–119.

Heim, A. and Chung, C.T., 1962. Preliminary observations on the structure of the Kaohsiung limestone mountains. Petroleum Geology of Taiwan, Jubilee Vol. King's 60th birthday, pp. 23–30.

Ho, C.S., 1986. A synthesis of the geologic evolution of Taiwan. Tectonophysics, 125: 1–16.

Lacombe, O., Angelier, J. and Laurent, P., 1993. Les macles de la calcite, marqueurs des compressions récentes dans un orogène actif: L'exemple des calcaires récifaux du sud de Taiwan. C. R. Acad. Sci., Paris, 316: 1805–1813.

Lacombe, O., Angelier, J., Rocher, M., Chen, H.-W., Chu, H.-T., Deffontaines, B., Hu, J.-C. and Lee, J.-C., 1995. Calcite twin analysis: a key to the recent stress fields at the front of the Taiwan collision belt. Symp. 'Active Collision of Taiwan', 22nd–23rd March, Taipei, Taiwan, pp. 157–166.

Laurent, P., 1984. Les macles de la calcite en tectonique: nouvelles méthodes dynamiques et premières applications. Thèse de Doctorat-ès-Sciences, Univ. Sci. Techn. Languedoc, Montpellier, 324 pp.

Lee, Y.-H., 1990. Nannobiostratigraphy, age correlation and paleoenvironments of the limestones in Kaohsiung area. Master thesis, Ntl. Sun Yat-Sen Univ., Kaohsiung, Taiwan (in Chinese).

Rocher, M., Lacombe, O., Angelier, J. and Chen, H.-W., 1996. Mechanical twin sets in calcite as markers of recent collisional events in a fold-and-thrust belt: Evidence from the reefal limestones of southwestern Taiwan. Tectonics, 15(5): 984–996.

Sun, S.C., 1963. The reef limestones and the geologic structures in the vicinity of Kaohsiung City, Taiwan. Special volume of Petroleum Geology of Taiwan for H.H. Ling's birthday, 2: 47–64.

Suppe, J., 1984. Kinematics of arc–continent collision, flipping of subduction, and back-arc spreading near Taiwan. Mem. Geol. Soc. China, 6: 21–34.